Letters in Applied NanoBioScience
Open-Access Journal (ISSN: 2284-6808)

Article
Volume 12, Issue 1, 2023, 23
https://doi.org/10.33263/LIANBS121.023

Function of ZnO Nanoparticles in the Remediation of the Toxic Metal, Seed Germination, and Seedling Growth of the Plant, Synthesized by Stem Extracts of *Anthophalus cadamba*

Shaik. Abdul Mathin [1,*], M. David Raju [2,*], D. Rama Sekhara Reddy [3]

[1] Research scholar of chemistry, Krishna University, Machilipatnam, AP, India
[2] Department of Chemistry, P.B.Siddhartha College of Arts and Sciences, Vijayawada, AP, India
[3] Department of Chemistry, Krishna University, Machilipatnam, AP, India
* Correspondence: abdulmathin786@gmail.com (S.A.M.), mdavidraju40@gmail.com (M.D.R.);
Scopus Author ID 57200092456 (S.A.M.)
6507847446 (M.D.R.)
Received: 20.11.2021; Accepted: 20.12.2021; Published: 10.01.2022

Abstract: The production of the Zinc oxide nanoparticles through aqueous stem extract of *Anthocephalus cadamba* Lin is performed. The formed nanoparticles tested for the toxic chromium metal removal activity, germination, and growth supporting of green gram seeds. The NPs were portrayed by FTIR, X-ray Diffraction, SEM, and EDX studies and confirmed irregular and complex structures. The % Chromium metal reduction of 87.83 %, 65.83 %, 48.00 % and 38.67 % was calculated at nanoparticle dosage of 1, 0.5, 0.25 and 0.10 g/L respectively. The amount of zinc accumulation in the roots of green gram was studied. The amount of Zn in the root tissue was increased significantly with the synthesized nanoparticles than zinc sulfate. It was observed that soil having ZnO-NPs shows the utmost rate of germination, root, and plant growth than with control and zinc sulfate.

Keywords: zinc oxide nanoparticles; chromium metal removal; green gram seed germination; plant growth activity.

1. Introduction

Nanotechnology is rapidly growing and making a big leap in nanoelectronics manufacturing. The nano applications spread in the health sector, medications, energy, biochemistry, and safety. The nanomaterials have a high surface-to-volume ratio, so they show characteristic nature than the properties of bulk materials. The metal NPs can be synthesized by different methods. Among them, plant extracts, algae, and fungi methods were ecofriendly, safe, dependable, and inexpensive paths to synthesize nanoparticles [1]. The industry effluents contain many heavy metallic materials, contaminating natural water resources. An occurrence of heavy metals, even at dilute concentrations in drinking water, will damage the health of human beings [2]. According to Indian standards (IS 10500: 2012), the chromium level in drinking water should be 0.05 mg/L. The heavy metals are not decomposed in the body. The omission of heavy metals in the water is necessary for human health. The adsorption, precipitation, membrane filtration, and ion-exchange methods were used to remediation heavy metals. Among these methods adsorption process to be efficient and economical for removing heavy metals [3]. Nanoparticles are entered into the environment through industrial goods and

inappropriate disposal of nanomaterials wastes which may restrain the germination of the seed and plant improvement [4,5]. The previous studies confirmed that nanoparticles had shown significant effects on the seed germination, seedling growth of mung, cucumber, spinach, tomato, and wheat [6-12]. The metal NPs also proved the improvement in the absorption of total nitrogen and content of micronutrients and also in the photosynthesis process. Synthesis of ZnO metallic NPs has been performed using the chemical and physical approach, i.e., reduction by hydrazine hydrate [13]; solvothermal method [14]; ultrasonic irradiation [15]. But these are nonenvironmental benign processes.

In the present study, the ZnO nanoparticles were synthesized from zinc acetate solution using *Anthocephalus cadamba* stem extracts. It is an ecofriendly process. Furthermore, synthesized NPs were tested to remove hexavalent chromium from the solution, seed germination, and plant growth activity.

2. Materials and Methods

2.1. Collection of plant material.

The *Anthocephalus cadamba* plant was available through the water channels, streams, and river banks. The plant was extended over Tamil Nadu, Andhra Pradesh, and Kerala in India. It can use as a decorative garden plant. The fresh plant was gathered from the local market of East Godavari, Andhra Pradesh, India [16]. The dirty parts of the plant were cleaned with wet filter paper. Then it was cut into small pieces and was dried in the shadow.

2.2 Preparation of aqueous leaf, stem, and root extracts Anthocephalus cadamba.

10 g of stem powder was mixed with 100 ml of Milli- Q water separately and kept on a water bath at 60°C for 20 min. The extract was cooled to room temperature and filtered using Whatman No.1 filter paper. The extract was kept in the refrigerator for further studies.

2.3. Green synthesis of zinc oxide nanoparticles.

According to Vijayakumar et al., 2018 the plant parts, i.e., leaves, stem, and root extracts, were studied separately to synthesize ZnO-NPsparticles. The Zinc Oxide nanoparticles were produced using a 0.01M Zinc acetate dihydrate solution. The 250 ml of Zinc acetate dihydrate solution was slowly mixed with 25 ml of the leaf, stem, and root extracts separately and heated at 60°C under a magnetic stirrer for 2 h. Then, the yellow color appeared and was allowed the mixture to settle for 8 h. The particles were centrifuged at 6000 rpm for 20 minutes, cleaned with distilled water, and then by methanol to eliminate wastes. Finally, powder of Zinc Oxide nanoparticles was obtained after overnight drying the purified precipitate at 80°C in a hot air oven.

2.4. Characterization of nanoparticles.

The crystalline arrangement of nanoparticles was portrayed through X-Ray Diffractometer at a scanning rate of 2 u angles/ min at 40 kV and 30 mA current. The scanning range was kept between 10^0 and 80^0 using Nickel monochromatic Cu Kα radiation (u = 1.5406 Å), NaI detector, variable slits, and 0.02 scan step size. The crystal size was measured using the Debye–Scherrer equation. Scanning electron microscopy (SEM) was used for morphological description and energy dispersive spectroscopy (EDS) to examine the elemental

account of metal nanoparticles. Fourier transform infrared spectroscopy (FTIR) investigates surface chemistry and organic functional groups. The FTIR was made by Bruker Company (Germany) with model ALPHA.

2.5. Metal adsorption study.

The competence of ZnO NPs to adsorb chromium ions was studied using the method described by Ghadah and Fawzan (2018). Potassium dichromate ($K_2Cr_2O_7$ analytical grade, Sigma Aldrich) and distilled water are used to make 1 g/L of chromium (VI) stock solution and the preferred concentrations from the stock solution. The adsorption experiments were carried out in a sequence of flasks containing 100 mL solutions of chromium metal ions at the desired concentration and mass of adsorbent (ZnO NPs). The mixtures were stirred for 24 h at 120rpm using an orbital shaker. The mixtures were filtered and calculated the concentrations of heavy metal. The effect of adsorbent doses of 0.1 g/L, 0.25 g/L, 0.50 g/L, and 1 g/L on the metal adsorption was studied.

2.5.1. Estimation of chromium by diphenylcarbazide (DPC) method.

According to Sanchez and Hofmann (2018), the DPC solution was prepared by mixing 0.02 g of 1, 5-diphenylcarbazide with 10 mL ethanol and 40 mL of 1.8 M sulfuric acid.

Table 1. Standard Calibration curve for the estimation of Chromium.

S No	Concentration in µg/ml	Average Absorbance
1	5	0.176
2	10	0.335
3	15	0.487
4	20	0.619
5	25	0.782
6	30	0.931

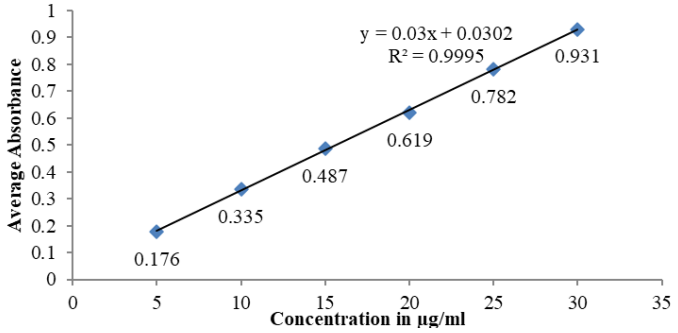

Figure 1. Standard Chromium calibration curve.

1.2 mL of DPC solution and 0.1 mL of concentrated nitric acid were added to 20 mL of the sample metal solution. A deep purple-colored complex comes into sight, and this one has the stability of 15 min only. Adsorption is measured at 560 nm wavelength. Linearity between absorbance and concentration is verified in the concentration range of 5 – 30 µg/mL. The absorbance-concentration calibration curve was plotted with a correlation coefficient, R^2, of 0.9995, shown in Table 1 and figure 1.

2.6. Seed germination and nurturing of plant growth.

2.6.1. Pot experiments.

Productive red soil was taken from the agricultural ground and was brought to the study location. The seeds of green gram (*Trigonella foenum-graecum* L.) were procured from the local market, Guntur. The soil was air-dried and was passed through a 1 cm sieve, and the Nitrogen (N), potassium (K), and phosphorus (P) content of the soil were evaluated in the soil. Plastic pots with 15 cm height and 45 cm diameter with a pot pad were filled with 1.25 kg soil. Some pots were homogenized with the ZnO-NPs at a dosage of 10 mg, 100 mg, 1000 mg/kg, respectively and other pots mixed with standard $ZnSO_4$ at 100 mg and 1000mg/kg for germination experiments with three replicates. The pot had soil without ZnO nanoparticles, and $ZnSO_4$ was also tested for germination. It is known as control. The soils were soothed with NPs before 24 h of the experiment. One hundred seeds were elected for germination, and observe the seedlings grew up to four leaves. Water was added at about 60 % of the maximum field capacity during the pot experiment work and harvested for 10 days. From the results observed, the germination rate (Germination rate (%) = number of germinated seeds/total seed number for testing × 100), root length, shoot length, and number of leaves per plant were calculated. The amount of Zn in the root tissue was calculated. The results of all treated samples were compared with respect to control. All of the experiments were done with three replicates, and results are presented as an average of the replicate analysis.

3. Results and Discussion

3.1. Synthesis of ZnO nanoparticles.

ZnO nanoparticles were produced by a green approach using aqueous stem extracts of *Anthocephalus cadamba* at room temperature. The primary phytochemical examination of aqueous extract from *Anthocephalus cadamba* exposed that the stem extract has more potential phytochemicals involved in forming ZnO nano from zinc acetate; table 2 and Figure 2. The color changed by metallic nanoparticles is due to the coherent excitation of all “free” electrons, which are released by the phenolic compounds present in the stem extracts. The number of tannins, polyphenols, and flavonoids present in the plant extracts are usually accountable for reducing metal compounds into their respective nanoparticles. The application of plant extracts in the making of nanoparticles is potentially valuable over microorganisms due to the ease of development and less biohazard nature [17].

3.2. Characterization of nanoparticles.

The characterization of nanoparticles is usually done based on their shape, size, surface area, and dispersion. Plant-based making of nanoparticles has been popular because the biosynthesized nanoparticles are uniform and stable. Thus, it could be used for its ample applications in various fields. However, nanoparticle size, shape, and formation differ among different plant species because of the reaction with metal ions and various biomolecules in the plant extract [18-20].

FTIR spectra of ZnO NPs (Figure 2) established an absorption band at 3707 cm^{-1} is supported the subsistence of Amide N-H Stretch or OH group in alcohol. Two medium groups were seen at 3426 and 3357 cm^{-1}. The 3707 cm^{-1} confirms critical amine gatherings. Strong bonds at 2998 and 2943 cm^{-1} point out C-H stretching vibrations. The bond at 1731 cm^{-1} indicates the C=O stretch vibrations in carbonyls. The 1367 cm^{-1} represents the C-N stretch in

amines in the IR spectra. The C=C bond stretching was seen at 1464 cm^{-1}. The FT-IR spectra of the synthesized nanoparticles are given in Figure 3.

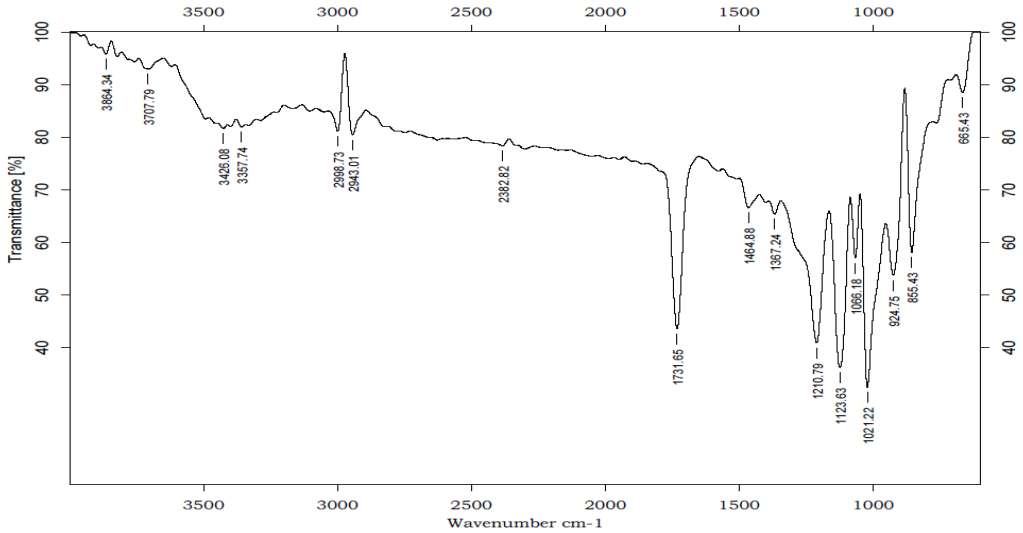

Figure 2. FT-IR spectra of synthesized ZnO NPs.

The crystalline size, shape, and surface morphology of the ZnO nanoparticles can be determined using SEM. The shape of the nanoparticle was found irregular and complex. The average molecule size was discovered to be 167nm. The micrograph images of ZnO nano express that they are in a nanoscale area and have a standardized round shape and less aggregation noticed. The SEM images of nanoparticles are shown in Figure 3.

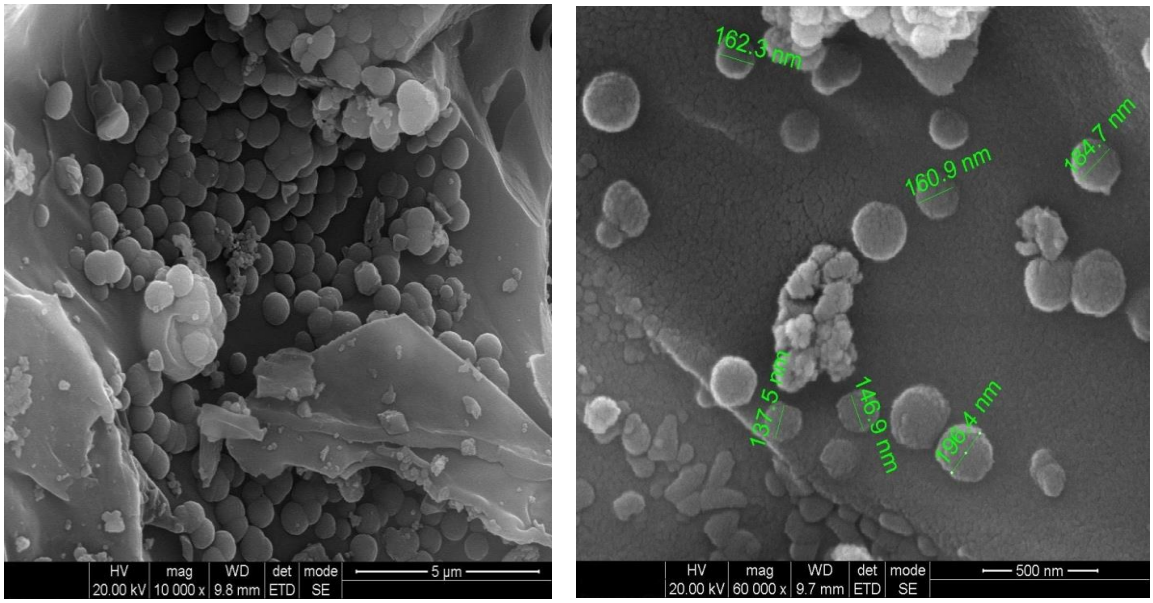

a) SEM image of NPs at 5-µm **b)** SEM image of NPs at 500 nm

Figure 3. SEM images of synthesized ZnO NPs.

The EDX pattern of the ZnO nano is shown in Figure 4. The C signal observed in EDX spectra is from the carbon film coated on the support. A characteristic signal resultant to Zn metal was observed in the spectra. No other signals were spotted within the exposure confines of EDS, which authenticate the purity of the ZnO nanoparticles. The percentage of Zn content in the crystalline particle was found to be 25.29%.

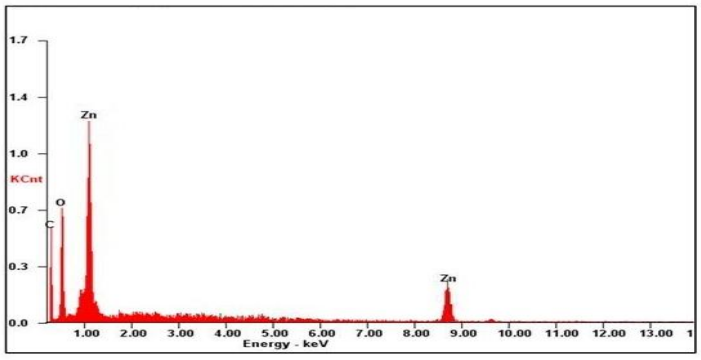

Element	Wt%	At%
CK	38.37	53.96
OK	26.34	37.91
ZnK	25.29	8.13
Matrix	Correction	ZAF

Figure 4. EDX results of synthesized ZnO NPs.

3.3. Metal adsorption study.

The capability of ZnO NPs to adsorb chromium ions was studied using the method described by Ghadah and Fawzan (2018) [21]. The adsorption of Chromium metal ions in solutions depended on the initial concentrations. In the present study, the initial metal concentrations from 10 to 200µg/mL were used for Cr metal adsorption by ZnO NPs. The initial concentration of *Cr* did not influence the percentage of *Cr* adsorption. Table 2 and Figure 5 show that the percentage adsorption of heavy metals increased when the initial metal concentration increased. The highest adsorption was detected at 100µg/mL with a 63.50 percent reduction.

Table 2. Optimization of initial concentration of Chromium metal.

S No	Concentration of Chromium (µg/ml)	Average Absorbance	Dilution Factor	Amount Estimated	% Reduction
1	10	0.311	1	93.67	6.33
2	25	0.608	1	77.07	22.93
3	75	1.527	1	66.53	33.47
4	100	1.125	1	36.50	63.50
5	150	0.497	5	77.83	48.11
6	200	0.765	5	122.50	38.75

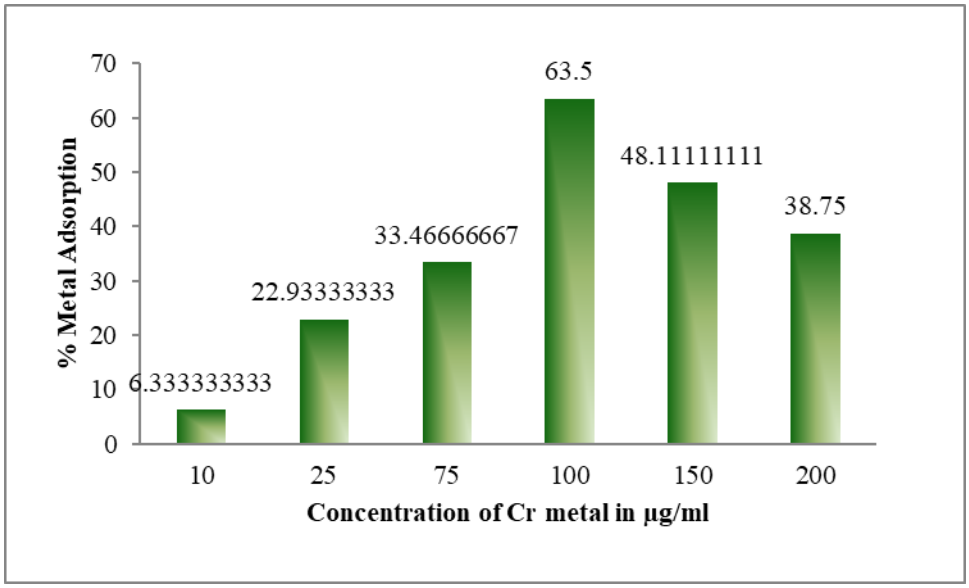

Figure 5. Optimization of initial concentration of Chromium metal.

The lowest adsorption of metals was observed with a high initial concentration of metals, i.e., at 200µg/mL with 38.75 percent chromium reduction. At high concentrations, the

competitive dispersion of metal ions has increased at the site available adsorbent surface; these pores are closed, and metal ions are prevented from passing deep into the adsorbent pores, which means that adsorption occurs only on the surface [22-24]. The effect of the optimization of the initial concentration of chromium metal for absorption and adsorbent doses and contact time on heavy metal adsorption was shown in Table 3. The adsorption percentage of chromium increased with adsorbent doses and contact time. The adsorption percentage increased with increasing the adsorbent dose and time because of the increased availability of surface area or many desorption sites or exchange sites at higher concentrations of adsorbents [25-28].

Table 3. % Reduction of Chromium metal using synthesized nanoparticles of different dosage

S No	Time in h	1 g/L	0.5 g/L	0.25 g/L	0.10 g/L
1	0	0.67	3.00	0.83	0.33
2	0.5	3.00	8.33	2.00	1.50
3	1	11.67	10.67	5.33	2.83
4	1.5	29.67	29.67	19.67	7.33
5	2	77.00	34.00	22.17	9.67
6	4	79.33	46.50	36.33	27.83
7	6	83.67	51.17	40.50	28.83
8	8	86.00	63.83	46.00	34.00
9	12	87.83	65.83	48.00	38.67

3.4. Sowing germination and fostering of plant growth.

Seed germination is the primary stage in plants' growth and plays a significant role all through the life cycle of plants. Thus the consequence of ZnO nanoparticles on the seed germination and plant growth of green gram was studied. Both nano ZnO and zinc sulfate influenced green gram germination dose-dependent. Green gram seed germination rates improved quickly in the initial days for all treatments, and at a dosage of less than 100 mg/ kg of ZnO-NPs and zinc sulfate shows less effect on the germination rate. The ZnO-NPs at a quantity of 1000 mg/Kg shows a very high germination rate of 98 %, whereas Zinc Sulfate at 1000 mg/Kg shows a significantly high germination rate of 79%. The germination of plants shows in Figure 6.

Figure 6. Germination of green gram plant of control, $ZnSO_4$ treated of 100 mg/kg , 1000 mg/kg and ZnO-NPs treated of 10 mg/kg , 100 mg/kg , 1000 mg/kg.

No significant inhibition of green gram seed germination in all the treatment conditions was observed. The germination rate results show in Table 4 and Figure 7.

Table 4. Germination rate (%).

S No	Sample studied	Germination rate (%)
1	Control	48
2	Zn Nano 10 mg/kg	65
3	Zn Nano 100 mg/kg	84
4	Zn Nano 1000 mg/kg	**98**
5	$ZnSO_4$ Treated 100mg/kg	58
6	$ZnSO_4$ Treated 1000mg/kg	79

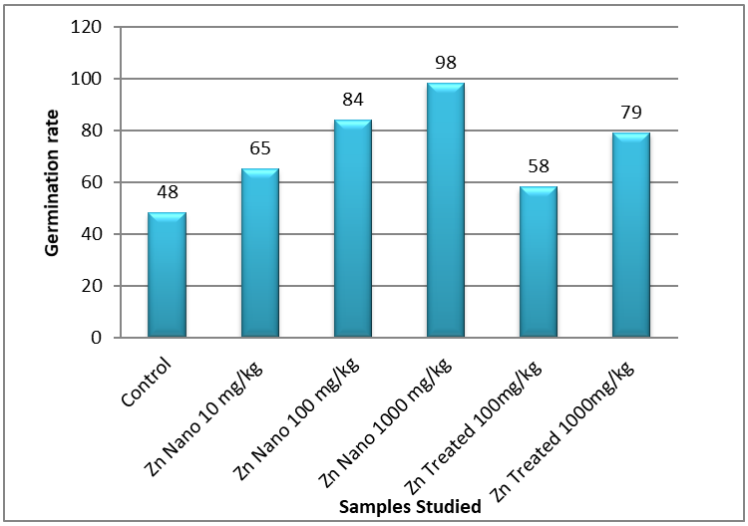

Figure 7. % Germination rate of seeds green gram plant.

Green gram seedling growth was determined by measuring the shoot length, root length, and the total number of leaves. In all the dosages, nanoparticles and zinc sulfate show a significant increase in root and shoot growth than the control. The average number of leaves was also found to be increased for the ZnO-NPs, and zinc sulfate treated plants. The root length of a green gram for the nanoparticles treated at a dosage of 1000 mg/kg (2.9 cm) increased significantly than the control (1.5 cm) and Zinc Sulphate 1000mg/Kg (2 cm). At the same time, the shoot length of a green gram for the nanoparticles treated at a dosage of 1000 mg/kg (11.2 cm) increased significantly than the control (8.7 cm) and Zinc Sulphate 1000mg/Kg (10.7 cm). Results of the pot experiment were given in Tables 5, 6, and Figure 8.

Table 5. Root Length of the plant.

S No	Sample studied	Root Length in cm
1	Control	1.5
2	Zn NPs 10mg/Kg	1.9
3	Zn NPs 100mg/Kg	2.1
4	Zn NPs 1000mg/Kg	**2.9**
5	Zinc Sulphate 100mg/Kg	1.9
6	Zinc Sulphate 1000mg/Kg	2

*Average of three replicate experiments

Table 6. Shoot Length of the plant.

S No	Sample studied	Shoot Length in cm
1	Control	8.7
2	Zn NPs 10mg/Kg	9.5
3	Zn NPs 100mg/Kg	10.9
4	Zn NPs 1000mg/Kg	**11.2**
5	Zinc Sulphate 100mg/Kg	9.8
6	Zinc Sulphate 1000mg/Kg	10.7

*Average of three replicate experiments

The gathering of Zn in root tissue was examined using Atomic Absorption Spectrophotometers. All the Zn nanoparticles and zinc sulfate treatments considerably increased the Zn concentrations and showed an increasing trend compared with control as doses increased. The Zn concentration in the root was 54.17 mg/kg in control, 241.76 mg/kg, and 139.71 mg/kg in the ZnO-NPs and zinc sulfate treatments, respectively. The zinc accumulation at a nanoparticles dose of 10 mg/kg, 100 mg/kg, and 1000 mg/kg was 107.48, 147.91, and 241.76 mg/Kg, respectively. In all the studies, concentrations of nanoparticles and zinc sulfate

were high compared with control. The zinc accumulation in the root was dose-dependent on the nanoparticle used for the treatment. The comparative study of the amount of zinc estimation in the root tissue of green gram was given in Table 7 and Figure 9.

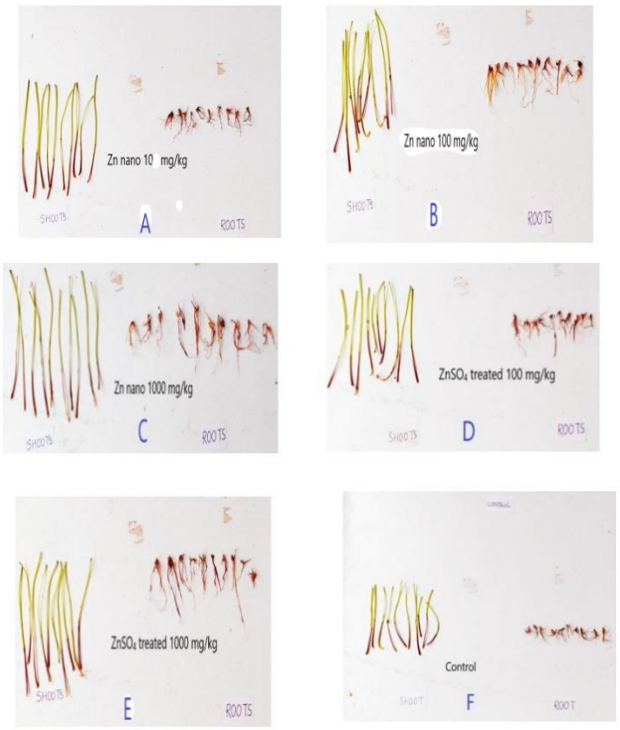

Figure 8. Comparison images of Shoot length and Root length of A) Zn nano 10 mg/kg; B) Zn nano 100 mg/kg; C) Zn nano 1000 mg/kg; D) $ZnSO_4$ treated 100 mg/kg; E) $ZnSO_4$ treated 1000 mg/kg; F) Control.

Table 7. Zinc accumulation in roots.

S No	Sample studied	Zinc accumulation in roots in mg/Kg
1	Control	54.17
2	Zn NPs 10mg/Kg	107.48
3	Zn NPs 100mg/Kg	147.91
4	Zn NPs 1000mg/Kg	**241.76**
5	Zinc Sulphate 100mg/Kg	99.18
6	Zinc Sulphate 1000mg/Kg	139.71

*Average of three replicate experiments

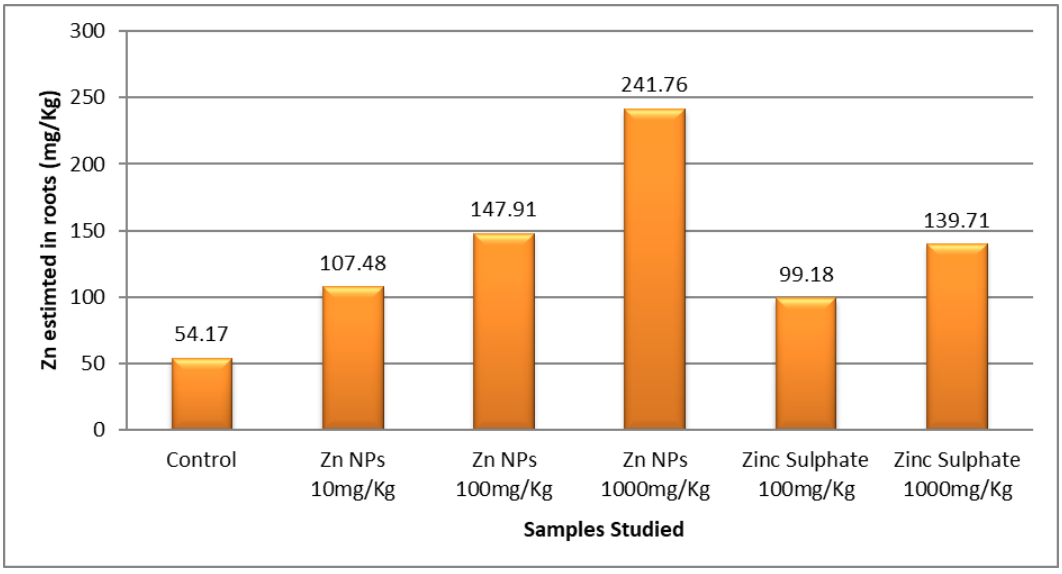

Figure 9. Comparative study of the amount of zinc estimation in the root tissue of green gram.

4. Conclusions

In this article, the adsorption potential of ZnO-NPsparticles synthesized using aqueous stem extract of *Anthocephalus cadamba* Lin was examined to exclude Cr (VI) in the aqueous solution. Further, the seed germination and plant growth effect of the nanoparticles were studied. The nitrogen-containing phytochemical components are concerned with the production of irregularly shaped nanoparticles and the average size of 167 nm with a zinc metal content of 25.29 %. The chromium metal removal efficiency of nanoparticles was observed to be more than 80 %, with an interaction time of 8 h. The synthesized nanoparticles were effectively promoted seed germination and plant growth.

Funding

This research received no external funding.

Acknowledgments

This research has no acknowledgment.

Conflicts of Interest

The authors declare no conflict of interest.

References

1. Soni, V.; Raizada, P.; Singh, P.; Cuong, H.N.; S, R.; Saini, A.; Saini, R.V.; Le, Q.V.; Nadda, A.K.; Le, T.-T.; Nguyen, V.-H. Sustainable and green trends in using plant extracts for the synthesis of biogenic metal nanoparticles toward environmental and pharmaceutical advances: A review. *Environmental Research* **2021**, *202*, https://doi.org/10.1016/j.envres.2021.111622.
2. Behzad, F.; Naghib, S.M.; kouhbanani, M.A.J.; Tabatabaei, S.N.; Zare, Y.; Rhee, K.Y. An overview of the plant-mediated green synthesis of noble metal nanoparticles for antibacterial applications. *Journal of Industrial and Engineering Chemistry* **2021**, *94*, 92-104, https://doi.org/10.1016/j.jiec.2020.12.005.
3. Castillo-Henríquez, L.; Alfaro-Aguilar, K.; Ugalde-Álvarez, J.; Vega-Fernández, L.; Montes de Oca-Vásquez, G.; Vega-Baudrit, J.R. Green Synthesis of Gold and Silver Nanoparticles from Plant Extracts and Their Possible Applications as Antimicrobial Agents in the Agricultural Area. *Nanomaterials* **2020**, *10*, https://doi.org/10.3390/nano10091763.
4. AlNadhari, S.; Al-Enazi, N.M.; Alshehrei, F.; Ameen, F. A review on biogenic synthesis of metal nanoparticles using marine algae and its applications. *Environmental Research* **2021**, *194*, https://doi.org/10.1016/j.envres.2020.110672.
5. Jurkow, R.; Pokluda, R.; Sękara, A.; Kalisz, A. Impact of foliar application of some metal nanoparticles on antioxidant system in oakleaf lettuce seedlings. *BMC Plant Biology* **2020**, *20*, https://doi.org/10.1186/s12870-020-02490-5.
6. Sayed Ahmed, H.I.; Elsherif, D.E.; El-Shanshory, A.R.; Haider, A.S.; Gaafar, R.M. Silver nanoparticles and Chlorella treatments induced glucosinolates and kaempferol key biosynthetic genes in Eruca sativa. *Beni-Suef University Journal of Basic and Applied Sciences* **2021**, *10*, https://doi.org/10.1186/s43088-021-00139-2.
7. Batool, S.U.; Javed, B.; Sohail; Zehra, S.S.; Mashwani, Z.-u.-R.; Raja, N.I.; Khan, T.; Alhaithloul, H.A.; Alghanem, S.M.; Al-Mushhin, A.A.M.; Hashem, M.; Alamri, S. Exogenous Applications of Bio-fabricated Silver Nanoparticles to Improve Biochemical, Antioxidant, Fatty Acid and Secondary Metabolite Contents of Sunflower. *Nanomaterials* **2021**, *11*, https://doi.org/10.3390/nano11071750.
8. Skiba, E.; Pietrzak, M.; Glińska, S.; Wolf, W.M. The Combined Effect of ZnO and CeO2 Nanoparticles on Pisum sativum L.: A Photosynthesis and Nutrients Uptake Study. *Cells* **2021**, *10*, https://doi.org/10.3390/cells10113105.
9. Rani, P.; Kaur, G.; Rao, K.V.; Singh, J.; Rawat, M. Impact of Green Synthesized Metal Oxide Nanoparticles on Seed Germination and Seedling Growth of Vigna radiata (Mung Bean) and Cajanus cajan (Red Gram). *Journal of Inorganic and Organometallic Polymers and Materials* **2020**, *30*, 4053-4062, https://doi.org/10.1007/s10904-020-01551-4.

10. Singh, Y.; Kaushal, S.; Sodhi, R.S. Biogenic synthesis of silver nanoparticles using cyanobacterium Leptolyngbya sp. WUC 59 cell-free extract and their effects on bacterial growth and seed germination. *Nanoscale Advances* **2020**, *2*, 3972-3982, https://doi.org/10.1039/D0NA00357C.
11. Itroutwar, P.D.; Kasivelu, G.; Raguraman, V.; Malaichamy, K.; Sevathapandian, S.K. Effects of biogenic zinc oxide nanoparticles on seed germination and seedling vigor of maize (Zea mays). *Biocatalysis and Agricultural Biotechnology* **2020**, *29*, https://doi.org/10.1016/j.bcab.2020.101778.
12. Baz, H.; Creech, M.; Chen, J.; Gong, H.; Bradford, K.; Huo, H. Water-Soluble Carbon Nanoparticles Improve Seed Germination and Post-Germination Growth of Lettuce under Salinity Stress. *Agronomy* **2020**, *10*, https://doi.org/10.3390/agronomy10081192.
13. Toqeer, I.; Raza, A.; Naz, M.Y.; Ghaffar, A.; Hussain, Z.; Ghuffar, A. Synthesis and application of controlled size copper oxide nanoparticles for improving biochemical and growth parameters of maize seedling. *Journal of Plant Nutrition* **2020**, *43*, 2622-2632, https://doi.org/10.1080/01904167.2020.1793182.
14. Wang, W.; Ren, Y.; He, J.; Zhang, L.; Wang, X.; Cui, Z. Impact of copper oxide nanoparticles on the germination, seedling growth, and physiological responses in Brassica pekinensis L. *Environmental Science and Pollution Research* **2020**, *27*, 31505-31515, https://doi.org/10.1007/s11356-020-09338-3.
15. Zhang, K.; Wang, Y.; Mao, J.; Chen, B. Effects of biochar nanoparticles on seed germination and seedling growth. *Environmental Pollution* **2020**, *256*, https://doi.org/10.1016/j.envpol.2019.113409.
16. Dwevedi, A.; Sharma, K.; Sharma, Y.K. Cadamba: A miraculous tree having enormous pharmacological implications. *Pharmacognosy reviews* **2015**, *9*, 107-113, https://doi.org/10.4103/0973-7847.162110.
17. Zhang, T.; Sun, H.; Lv, Z.; Cui, L.; Mao, H.; Kopittke, P.M. Using Synchrotron-Based Approaches To Examine the Foliar Application of ZnSO(4) and ZnO Nanoparticles for Field-Grown Winter Wheat. *J Agric Food Chem* **2018**, *66*, 2572-2579, https://doi.org/10.1021/acs.jafc.7b04153.
18. Zhang, R.; Zhang, H.; Tu, C.; Hu, X.; Li, L.; Luo, Y.; Christie, P. Phytotoxicity of ZnO nanoparticles and the released Zn(II) ion to corn (Zea mays L.) and cucumber (Cucumis sativus L.) during germination. *Environmental science and pollution research international* **2015**, *22*, 11109-11117, https://doi.org/10.1007/s11356-015-4325-x.
19. Lin, D.; Xing, B. Phytotoxicity of nanoparticles: inhibition of seed germination and root growth. *Environmental pollution (Barking, Essex:1987)* **2007**, *150*, 243-250, https://doi.org/10.1016/j.envpol.2007.01.016.
20. Fageria, P.; Gangopadhyay, S.; Pande, S. Synthesis of ZnO/Au and ZnO/Ag nanoparticles and their photocatalytic application using UV and visible light. *RSC Advances* **2014**, *4*, 24962-24972, https://doi.org/10.1039/C4RA03158J.
21. Al-Senani, G.M.; Al-Fawzan, F.F. Study on Adsorption of Cu and Ba from Aqueous Solutions Using Nanoparticles of Origanum (OR) and Lavandula (LV). *Bioinorganic Chemistry and Applications* **2018**, *2018*, 1-8, https://doi.org/10.1155/2018/3936178.
22. Liu, H.R.; Shao, G.X.; Zhao, J.F.; Zhang, Z.X.; Zhang, Y.; Liang, J.; Liu, X.G.; Jia, H.S.; Xu, B.S. Worm-Like Ag/ZnO Core–Shell Heterostructural Composites: Fabrication, Characterization, and Photocatalysis. *The Journal of Physical Chemistry C* **2012**, *116*, 16182-16190, https://doi.org/10.1021/jp2115143.
23. Kalishwaralal, K.; Deepak, V.; Ram Kumar Pandian, S.; Kottaisamy, M.; BarathManiKanth, S.; Kartikeyan, B.; Gurunathan, S. Biosynthesis of silver and gold nanoparticles using Brevibacterium casei. *Colloids and Surfaces B: Biointerfaces* **2010**, *77*, 257-262, https://doi.org/10.1016/j.colsurfb.2010.02.007.
24. Ahmed, S.; Ahmad, M.; Swami, B.L.; Ikram, S. A review on plants extract mediated synthesis of silver nanoparticles for antimicrobial applications: A green expertise. *Journal of Advanced Research* **2016**, *7*, 17-28, https://doi.org/10.1016/j.jare.2015.02.007.
25. Ashokkumar, S.; Ravi, S.; Kathiravan, V.; Velmurugan, S. Synthesis of silver nanoparticles using A. indicum leaf extract and their antibacterial activity. *Spectrochimica acta. Part A, Molecular and biomolecular spectroscopy* **2015**, *134*, 34-39, https://doi.org/10.1016/j.saa.2014.05.076.
26. Swamy, M.K.; Akhtar, M.S.; Mohanty, S.K.; Sinniah, U.R. Synthesis and characterization of silver nanoparticles using fruit extract of Momordica cymbalaria and assessment of their in vitro antimicrobial, antioxidant and cytotoxicity activities. *Spectrochimica acta. Part A, Molecular and biomolecular spectroscopy* **2015**, *151*, 939-944, https://doi.org/10.1016/j.saa.2015.07.009.
27. Al-Senani, G.M.; Al-Fawzan, F.F. Adsorption study of heavy metal ions from aqueous solution by nanoparticle of wild herbs. *The Egyptian Journal of Aquatic Research* **2018**, *44*, 187-194, https://doi.org/10.1016/j.ejar.2018.07.006.
28. Sanchez-Hachair, A.; Hofmann, A. Hexavalent chromium quantification in solution: Comparing direct UV–visible spectrometry with 1,5-diphenylcarbazide colorimetry. *Comptes Rendus Chimie* **2018**, *21*, 890-896, https://doi.org/10.1016/j.crci.2018.05.002.